TEMPERATURE DEPENDENCE OF THE KINETIC COEFFICIENTS OF $Bi_{0.94}Sb_{0.06}$ ALLOY

A.A. MUSAYEV[1], E.R. YUZBASHOV[2]
[1]National Aviation Academy, Mardakan av. 30, Baku, Azerbaijan
[2]Institute of Physics NAS Azerbaijan, H.Javid av. 131, AZ1143, Baku, Azerbaijan,
e-mail: eltaj100@yahoo.com

The temperature dependence (in the 78K–300*K* range) of the following components of the tensor of electric resistance in low magnetic field–two components of specific resistance (ρ_{11} and ρ_{33}), two components of Hall effect (R_{231} and R_{123}) and, five components of magnetoresistance ($\rho_{11,11}$, $\rho_{11,22}$, $\rho_{11,33}$, $\rho_{33,11}$, $\rho_{33,33}$) – for the alloy of $Bi_{0.94}Sb_{0.06}$ were measured. Due to the calculations the following kinetic parameters were determined: carrier densities of electrons *N* and holes *P*; their mobilities μ_1, μ_2, μ_3 and ν_1, ν_3, correspondingly; and the tilt angle of electronic isoenergetic ellipsoids to the bisectrix axis (φ_e). Calculations were carried out for two- (*L* electrons and *T* holes) and three-band (*L* electrons, *T* and *L* holes) models.

Keywords: semimetals, galvanomagnetic properties, kinetic coefficients of Bi-Sb alloys
PACS:72.15. Gd, 73.50.Jt

INTRODUCTION

Investigation of solid solutions of $Bi_{1-x}Sb_x$ displays that those solutions are perspective materials system for fundamental materials science, condensed matter physics, low temperature thermoelectrics, infrared applications, and beyond. Moreover, those materials are of broad interest from the theoretical aspect. Due to the smallness of the characteristic energetic parameters of solid solutions of Bi-Sb, those materials are very sensitive to the external impacts (temperature, pressure, presence of electroactive impurities, defects, etc.). By varying external influence in comparatively small range, it is possible to investigate topology of Fermi surface, various phase transitions, alter the statistics of charge carriers in rather broad range etc. That is why these materials are still being investigated as bulk materials, thin films and nanoscale structures [1]. Since then, different types of nano-structured $Bi_{1-x}Sb_x$ materials, have notably drawn the attention of researchers, including nanowires [2], thin films [3], and nano-particles [4]. Also, it was predicted that different kinds of Dirac cone systems can be synthesized based on the single crystal $Bi_{1-x}Sb_x$ thin films materials, including single-Dirac-cone, bi-Dirac-cone, tri-Dirac-cone, exact-Dirac-cone, semi-Dirac-cone, and quasi-Dirac-cone, and also including Dirac cones with different anisotropic degrees [5]. Fu and Kane predicted the topological insulator phase in $Bi_{1-x}Sb_x$ surface states [6], which is experimentally proved by Hsieh et al. [7]. These discover in $Bi_{1-x}Sb_x$ surface states directly leads to the intensively focused area of topological insulator [8], which promises potential applications in spintronics, superconductivity, quantum computing, etc.

In the early years, researchers found that the variation of the electronic band structure of bulk $Bi_{1-x}Sb_x$ provided a remarkable richness of electronic properties, when considered as a function of stoichiometry, temperature, strain, pressure, etc. Semimetals, direct band gap semiconducting and indirect band gap semiconducting behaviors have all been observed in this materials class. Furthermore, both parabolically and non-parabollically dispersed charge carriers can be found in this materials class. The high degree of anisotropy in their transport properties also distinguishes the $Bi_{1-x}Sb_x$ materials from other systems.

The electronic transport properties of bulk $Bi_{1-x}Sb_x$ have been studied in great detail. The most interesting phenomenon for bulk $Bi_{1-x}Sb_x$ materials is that when $x<0.04$ the *L*-point band gap decreases with antimony composition x, while when $x>0.04$ the *L*-point band gap increases with antimony composition *x* (fig.1). At $x=0.04$ the conduction band edge and the valence band edge exchange their symmetries at the *L* points, and the *L*-point band gap E_{gL} becomes zero, which leads to the formation of three symmetrical three-dimensional (*3D*) Dirac points [9].

In itself studying the transport phenomena in the system of Bi-Sb represents a powerful tool for investigating energetic zone structure and mechanisms of scattering of charged carriers in these materials. But studying galvano-and thermomagnetic effects in these materials at intermediate (*77K-300K*) and high (more than room temperature) temperatures become irreplaceable, because the best powerful methods for investigating energetic zone structure and mechanisms of scattering of charged carriers, as oscillation and resonance methods, are effective only at ultra- and low temperatures.

EXPERIMENT

Investigation of temperature dependence of low-field galvanomagnetic coefficients of the alloy of $Bi_{0.94}Sb_{0.06}$ at the temperature range of 78÷300*K* was carried out in the paper. Single crystals of $Bi_{0.94}Sb_{0.06}$ were grown by the method of Chokhralsky in the experimental equipment [10] using solid replenishment.

131, H.Javid ave, AZ-1143, Baku
ANAS, Institute of Physics
E-mail: jophphysics@gmail.com

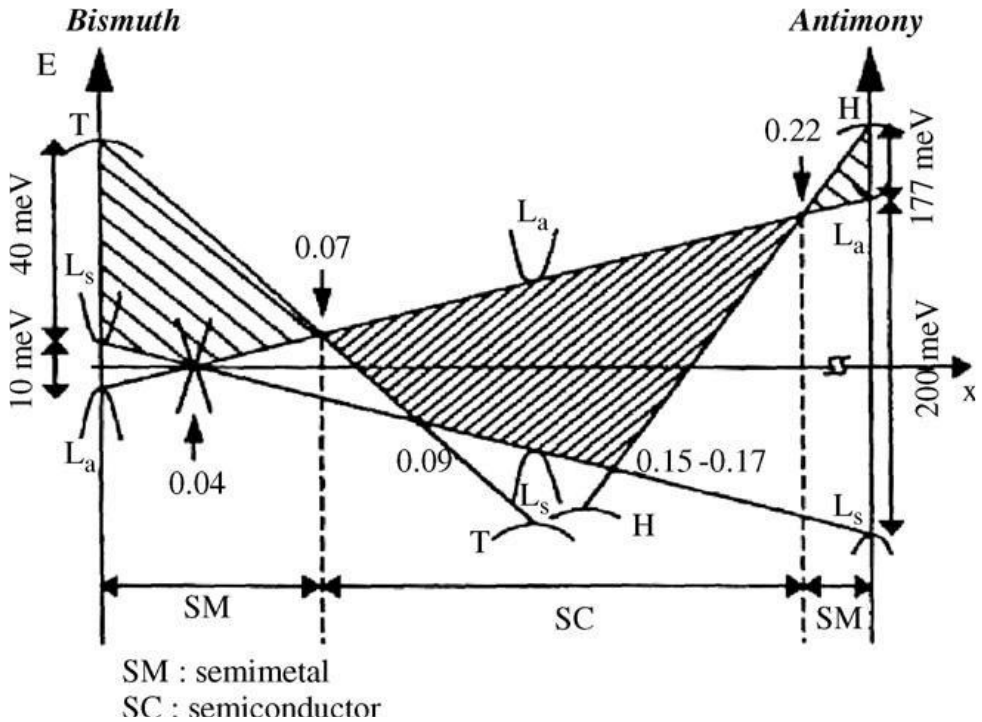

Fig. 1. Schematic representation of the energy bands near the Fermi level for $Bi_{1-x}Sb_x$ alloys as a function of x at $T=0K$.

Two types of rectangular samples were cut from the single crystal ingot by electrospark method; large edges of the first group of samples were parallel to binary axe, but the second group ones were aligned parallel to trigonal axe. For diminution of influence of parasite thermomagnetic effects on the precision of measurement of isothermal galvanomagnetic coefficients, the measurements were carried out in special module filled with helium. Due to the precautions the temperature gradient between contact points was reduced up to 0.03 ÷ 0.05 K. For reducing of thermal leakage over measuring wires and thermocouples were used thin ones (having diameter less than 0.1mm). All measuring wires and thermocouples were thermostateted. Calculation of the wires' length was carried out according to the work [11]. As known during the measurement of specific resistance of a thermoelectrical specimen an additional error makes its appearance due to the Peltier effect. But using a fast-acting, precious digital voltmeter allows to make this error negligible. The measurement of other galvanomagnetic coefficients were conducted by the high-precious D.C. Potentiometer. In every case the fulfillment of the low-field condition ($\mu B << 1$) were tested, because this varies in the rather broad range depending on temperature and orientation of magnetic field with respect to main crystallographic axes (usually its magnitude not exceeds 0.02÷0.04 Tesla at nitrogen temperatures).

The following components of the tensor of electric resistance in low magnetic field for the alloy of $Bi_{0.94}Sb_{0.06}$ - two components of specific resistance (ρ_{11} and ρ_{33}), two components of Hall effect (R_{231} and R_{123}) and, five components of magnetoresistance ($\rho_{11,11}$, $\rho_{11,22}$, $\rho_{11,33}$, $\rho_{33,11}$, $\rho_{33,33}$) – were measured. These coefficients are defined conveniently with respect to the usual orthogonal coordinate system used for the trigonal semimetals Bi, Sb, having 1 along the binary (x) axis, 2 along the bisectrix (y) axis and 3 along the trigonal (z) axis (fig. 2).

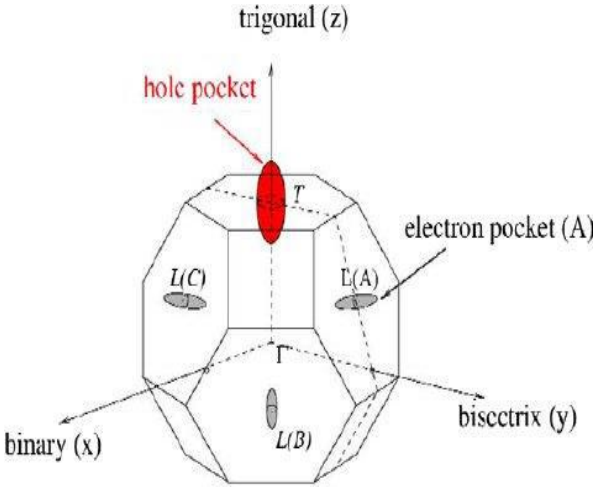

Fig. 2. The Brillouin zone of Bi and Bi-rich alloys showing three L-point electron pockets and one T-point hole pocket.

The dependence of components of specific resistance (ρ_{11} and ρ_{33}) on temperature at the investigated temperature range showed metallic character (fig.3). The temperature dependences of the Hall and magnetoresistance coefficients are shown in the figures 4 and 5, correspondingly.

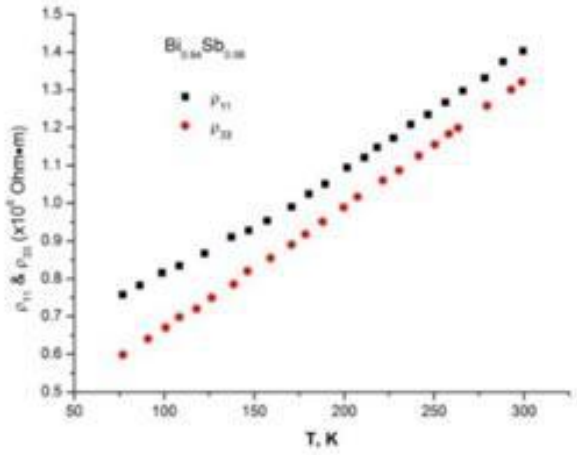

Fig. 3. Temperature dependence of isothermal specific resistivities ρ_{11} and ρ_{33}.

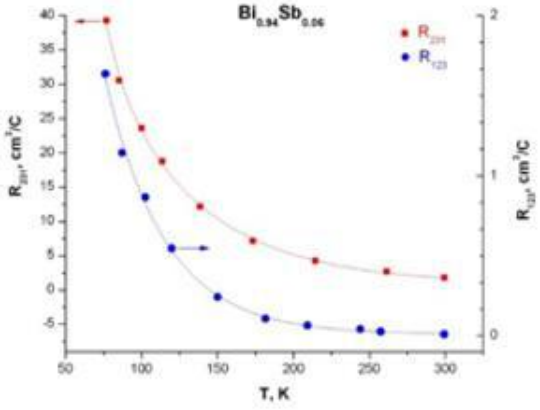

Fig. 4. Temperature dependence of Hall coefficients R_{231} and R_{123}.

From the figure 4 it is clear that both Hall components greatly decrease with temperature. Such decreasing may be caused by increasing of the concentration of charge carriers. However, as the conductance of Bi-Sb alloys is intrinsic at the given temperature range, the changes of Hall coefficients may be related to the alteration of ratio of mobilities of electrons and holes. Therefore, the temperature dependence of Hall coefficients cannot quantitatively characterize alteration of the concentration of current carriers and more complicated calculations considering of adopted model of energetic spectra must be conducted.

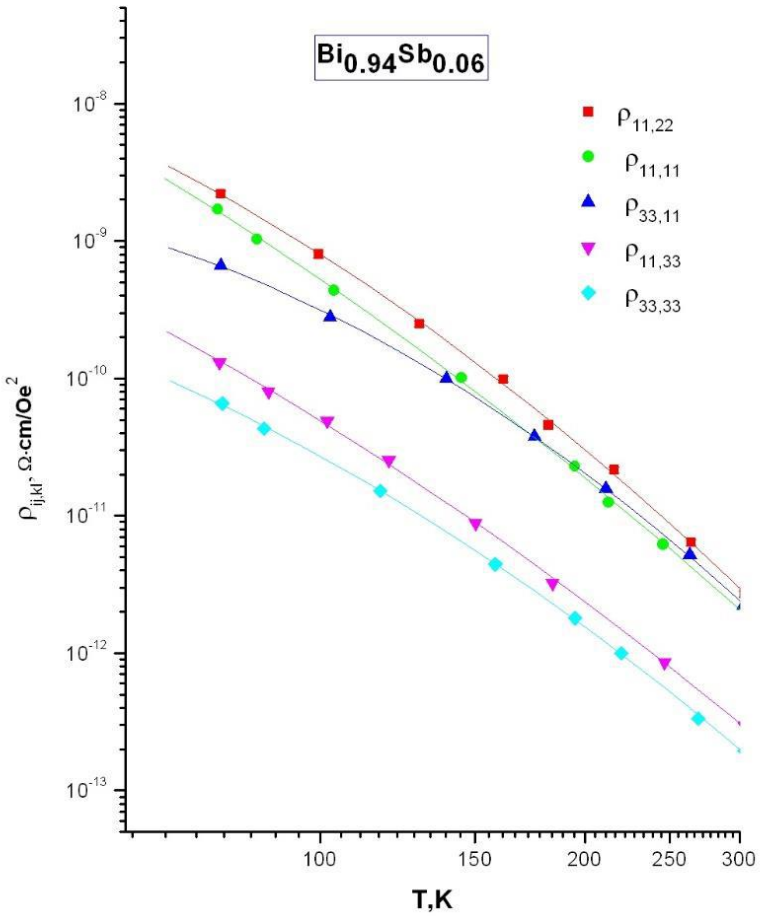

Fig. 5. Temperature dependence of five components of magnetoresistance in double-logarithmic scale.

From the figure 5 it is clear that common features of the temperature dependences of all measured components of magnetoresistance are identical. Each line representing the dependence of $lg\ \rho_{ij,kl}$ on $lg\ T$ may be considered as two nearly linear sections: low-temperature section (from 78*K* to 120÷160*K*) which monotonically turn into high-temperature section (from 160 ÷ 200K to 300K). These dependences bear exponential character ($\rho_{ij,kl} \sim T^{-P}$), and index of power P is greater at the high-temperature section than at low-temperature one, and its value depends on the direction of a component.

RESULTS AND CALCULATIONS

For the quantitative interpretation of the obtained experimental results, it is needed to adopt appropriate models for energetic band structure and theoretical approximations for calculation kinetic coefficients for BiSb alloys. It is known that in anisotropic mediums, such as Bi, Sb and their solid solutions, with point-group symmetry $R\bar{3}m$, the fundamental equation for the conduction of electricity in a magnetic field *B* is the generalized form of Ohm's law relating the current density *J* to the applied field *E*:

$$J_i = \sigma_{ij}(B)E_j \quad \text{or} \quad E_i = \rho_{ij}(B)J_j \tag{1}$$

where the resistivity tensor $\rho_{ij}(B)$ is the reciprocal of the conductivity tensor $\sigma_{ij}(B)$; both are general functions of B and obey the Onsager relation [$\rho_{ij}(B) = \rho_{ij}(-B)$].

Transport phenomena are expressed by the Boltzmann equation. If $\mu B << 1$ (μ is the carrier mobility) the solution in the form of power series in *B* will converge rapidly and only terms to B^2 are required to explain the galvanomagnetic effects in low magnetic fields. Accordingly, $\rho_{ij}(B)$ is defined as follows:

$$\rho_{ij}(B) = \rho_{ij} + R_{ijk}B_k + \rho_{ijkl}B_kB_l \tag{2}$$

While the magnetoresistivity tensor is measured experimentally, theory is more conveniently handled in terms of magnetoconductivity tensor. The formulae that transform from one tensor to the other are the following:

$$\left.\begin{aligned} \sigma_{11} &= \frac{1}{\rho_{11}}; & \sigma_{33} &= \frac{1}{\rho_{33}} \\ \sigma_{123} &= \frac{R_{123}}{\rho_{11}^2}; & \sigma_{231} &= \frac{R_{231}}{\rho_{11}\rho_{33}} \\ \sigma_{1111} = \frac{\rho_{1111}}{\rho_{11}^2}; \quad \sigma_{1122} &= \frac{\rho_{1122}}{\rho_{11}^2} + \frac{R_{231}^2}{\rho_{11}^2\rho_{33}}; \quad \sigma_{1133} = \frac{\rho_{1133}}{\rho_{11}^2} + \frac{R_{123}^2}{\rho_{11}^3} \\ \sigma_{3333} &= \frac{\rho_{3333}}{\rho_{33}^2}; & \sigma_{3311} &= \frac{\rho_{3311}}{\rho_{33}^2} + \frac{R_{231}^2}{\rho_{33}^2\rho_{11}} \end{aligned}\right\} \tag{3}$$

The magnetoconductivity tensor components of a semimetal of crystal class $R\bar{3}m$ with a many-valley band structure are related to the principal carrier mobilities μ_i and ν_i (where *i* is l, 2, 3) of electrons and holes respectively by a set of equations. The concrete kind of the set of equations depends on the considered model of energetic band structure extrema laid near Fermi level. In our case according to the Fermi surface peculiarities (fig. 2) of charge carries we have taken into the account 3 electron and hole ellipsoids (pockets) localized at L point of the *BZ* and heavy holes localized at *T* point. The important assumptions are independent contribution to electric current from each valley and an isotropic relaxation time in k-space. So, $\sigma(\vec{B}) = \sum_s \sigma_s(\vec{B})$. Here $\sigma_s(\vec{B})$ is the contribution of *s* valley to the common electrical conductivity. In our calculations we considered two models for the $Bi_{0.94}Sb_{0.06}$ alloy:

$$\sigma(\vec{B}) = 3\sigma_s^e(L) + \sigma_s^h(T) \tag{4}$$

and

$$\sigma(\vec{B}) = 3\sigma_s^e(L) + \sigma_s^h(T) + 3\sigma_s^h(L) \tag{5}$$

The set of the equations connecting the magnetoconductivity tensor components with kinetic parameters in our case may be expressed for one ellipsoid as the following:

$$\sigma_{11} = \frac{1}{2}Ne[\mu_1 + C^2\mu_2 + S^2\mu_3]$$
$$\sigma_{33} = Ne[S^2\mu_2 + C^2\mu_3]$$
$$\sigma_{231} = \frac{1}{2}Ne[\mu_2\mu_3 + \mu_1(S^2\mu_2 + C^2\mu_3)]$$
$$\sigma_{123} = Ne[\mu_1(C^2\mu_2 + S^2\mu_3)]$$

$$\sigma_{1133} = \frac{1}{2}Ne[\mu_1(\mu_1 + C^2\mu_2 + S^2\mu_3)(C^2\mu_2^2 + S^2\mu_2^2)]$$

$$\sigma_{3311} = \frac{1}{2}Ne\left[(S^2\mu_1 + C^2\mu_3) + [\mu_2\mu_3 + \mu_1(S^2\mu_2 + C^2\mu_3]\right]$$

$$\sigma_{1111} = \frac{1}{8}Ne[S^2\mu_2(\mu_1 - \mu_3)^2 + C^2\mu_3(\mu_1 - \mu_2)^2 + 3S^2C^2\mu_1(\mu_2 - \mu_3)]$$

$$\sigma_{1122} = \frac{1}{8}Ne[3S^2\mu_2(\mu_1^2 + \mu_3^2) + 3C^2\mu_3(\mu_1^2 + \mu_2^2) + C^2S^2\,\mu_1(\mu_2 - \mu_3)^2 + 2\mu_1\mu_2\mu_3]$$

$$\sigma_{3333} = Ne[C^2S^2\,\mu_1(\mu_2 - \mu_3)^2]$$

Here: $S=\sin\varphi$, $C=\cos\varphi$; φ is the tilt angle of the energetic ellipsoid to the basis surface; for *L*-type charge carriers $\varphi_e(L)=\varphi_h(L)$; for *T*-holes $\varphi_h(T)=0$. So, for heavy holes $S=0$ and $C=1$and $\nu_1=\nu_2$, because *T*-ellipsoid is an ellipsoid of revolution.

To obtain a fairer assessment of the experimental data, a computer program producing a least-mean-squares best fit to all nine coefficients were devised. Due to the calculations the following kinetic parameters were determined: carrier densities of electrons *N* and holes P; their mobilities μ_1, μ_2, μ_3 and ν_1, ν_3, correspondingly; and the tilt angle of electronic isoenergetic ellipsoids to the bisectrix axis (φ_e). It should be noted that not all of these parameters were determined with the same accuracy. The most preciously were determined *N*, *(P)*, μ_1, μ_3 and ν_1. The contribution of μ_2 is small and is almost swamped by μ_1, and μ_3. The solution shown in the Table 1 was obtained for the case of equality the carrier densities of electrons *N* to carrier densities of holes *P*, localized at *T*-point of the Brillouin zone.

Table 1.

Calculated kinetic parameters of $Bi_{0.94}Sb_{0.06}$ alloy obtained for model $N_L=P_T$

T	*N=P*	φ_e	μ_1	μ_2	μ_3	ν_1	ν_3
(K)	*(m^{-3})*	*(deg)*	*($m^2/V\cdot s$)*	*($m^2/V\cdot s$)*	*($m^2/V\cdot s$)*	*($m^2/V\cdot s$)*	*($m^2/V\cdot s$)*
78	$1.10\cdot10^{23}$	6.41	119	0.65	82.3	9.44	14.6
90	$1.43\cdot10^{23}$	6.58	94.3	0.54	55.0	7.60	12.9
110	$2.04\cdot10^{23}$	7.08	62.9	0.38	34.3	5.31	8.0
130	$2.85\cdot10^{23}$	6.75	45.6	0.24	22.2	3.75	5.27
150	$3.74\cdot10^{23}$	7.29	32.3	0.16	15.1	2.80	4.1
170	$4.89\cdot10^{23}$	6.99	23.9	0.1	10.2	2.11	3.1
190	$6.26\cdot10^{23}$	6.99	17.8	0.076	7.4	1.60	2.2
210	$7.75\cdot10^{23}$	7.62	13.5	0.055	5.5	1.31	1.8
250	$1.23\cdot10^{24}$	7.67	7.6	0.036	3.1	0.76	0.95
270	$1.48\cdot10^{24}$	7.9	6.0	0.031	2.4	0.62	0.77
300	$1.99\cdot10^{24}$	7.9	4.0	0.024	1.7	0.45	0.46

The result of calculations for the case of equality carrier densities of electrons N to the sum of carrier densities of heavy holes localized at *T*- and light holes at *L*- points of the Brillouin zone (i.e. $N_L=P_L+P_T$) is shown in the table 2**.**

Table 2.

Calculated kinetic parameters of $Bi_{0.94}Sb_{0.06}$ alloy obtained for model $N_L=P_T+P_L$

T	*N*	P_T	P_L	*R*	μ_1	μ_2	μ_3	ν_1
(K)	*(m^{-3})*			*(%)*	*($m^2/V\cdot s$)*	*($m^2/V\cdot s$)*	*($m^2/V\cdot s$)*	*($m^2/V\cdot s$)*
78	$1.19\cdot10^{23}$	$1.14\cdot10^{23}$	$0.05\cdot10^{23}$	4.4	114.2	0.47	83.1	6.61
90	$1.56\cdot10^{23}$	$1.47\cdot10^{23}$	$0.08\cdot10^{23}$	5.6	82.9	0.46	58.6	5.80
110	$2.25\cdot10^{23}$	$2.10\cdot10^{23}$	$0.15\cdot10^{23}$	6.5	53.7	0.36	37.7	4.21
130	$3.11\cdot10^{23}$	$2.88\cdot10^{23}$	$0.23\cdot10^{23}$	7.34	37.1	0.25	24.5	3.12
150	$4.07\cdot10^{23}$	$3.75\cdot10^{23}$	$0.32\cdot10^{23}$	7.9	27.3	0.18	17.1	2.50
170	$5.31\cdot10^{23}$	$4.85\cdot10^{23}$	$0.46\cdot10^{23}$	8.66	19.9	0.13	11.7	1.91
190	$6.77\cdot10^{23}$	$6.16\cdot10^{23}$	$0.61\cdot10^{23}$	9.0	14.9	0.096	8.4	1.40
210	$8.37\cdot10^{23}$	$7.57\cdot10^{23}$	$0.80\cdot10^{23}$	9.6	11.5	0.079	6.3	1.11
250	$1.31\cdot10^{24}$	$1.18\cdot10^{24}$	$1.27\cdot10^{23}$	9.7	6.7	0.052	3.5	0.70
270	$1.58\cdot10^{24}$	$1.43\cdot10^{24}$	$1.51\cdot10^{23}$	9.6	5.4	0.047	2.7	0.58
300	$2.09\cdot10^{24}$	$1.92\cdot10^{24}$	$1.71\cdot10^{23}$	8.2	3.9	0.035	1.9	0.44

In this calculation the tilt angle of electronic isoenergetic ellipsoids to the bisectrix axis (φ_e) was chosen as a constant equaled to $6^0 40''$. This assumption is valid, because in the temperature range studied the alteration of φ_e does not greatly affect to the result of the calculation. Further the calculations indicated that as the temperature increases the results of the calculation are less sensitive to the value of ν_3. So, the data for ν_3 is not cited, because an accurate value of it cannot be obtained.

The table 2 shows that a contribution of light holes P_L into the total hole conductivity ($P=P_L+P_T=N$) increases as the temperature rises, but a relative contribution of light holes to the total hole conductivity R [$R=P_L/(P_L+P_T)$] has a maximum at the temperature about 250K. Such dependence may be explained, if we take into account that in the narrow-gap semimetals as Bi-Sb the energetic gap E_g, in the first approximation, is increasing in quadratic law [12], but activation thermal energy in linear law by the increasing of temperature. Therefore, a contribution of light holes P_L decreases as the temperature rises in the range of high temperatures.

Taking into the account that formulas connecting $\rho_{ij,kl}$ with kinetic coefficients in each concrete case contain different combinations of μ_i, ν_i and the temperature dependencies of above mentioned parameters, strictly speaking, do not expressed as exponential functions, then there is good reason to believe that determined temperature dependencies of kinetic parameters are reasonable.

One of the factors leading to the strong temperature dependencies of the magnetoresistivity coefficients is the strong temperature dependence of mobility ($\mu \sim T^{-3}$). Such strong dependence of mobility cannot be explained only by scattering of current carriers on intravalley acoustic phonons. It is possible that intervalley scattering by optical phonons may play active role at high temperatures. It should be noted that alteration of the effective mass of current carriers might make contribution to the strong temperature dependency of the mobility.

It is clear that to calculate the temperature dependences of all kinetic parameters of $Bi_{1-x}Sb_x$ solid solutions in more precious manner, taking into account the complex nature of the energy band structure, dispersion law of charge carriers, a sharp temperature dependence of the energy gaps and the effect effective masses of charge carriers, features of energy ellipsoids and scattering mechanisms (anisotropic case), is very difficult task. But, due to the lack of reliable parameters for estimation purposes are commonly used simple models. In addition, when looking for suitable materials for thermoelectric converters, it is often enough to know the average kinetic parameters for single crystals or parameters for polycrystalline samples of the same composition.

Hence, the use of polycrystalline materials might be more suitable for practical applications (because single crystals are weak in mechanical strength and require dedicated techniques for synthesis). But there are very limited reports on transport property study of polycrystalline Bi-Sb alloys [13,14].

In our case, to estimate the values of some kinetic coefficients, it is sufficient to use the average value of the measured galvanomagnetic coefficients.

For this, we used the following general formulas for resistivity, Hall effect and magnetoresistance, respectively [15]:

$$\left.\rho = \frac{1}{3}(2\rho_{11} + \rho_{33})\,;\; R = \frac{1}{3}(2R_{231} + R_{123})\,;\; \frac{\delta\rho}{B^2} = \frac{1}{15}(\rho_{1111} + 5\rho_{1122} + 4\rho_{1133} + 4\rho_{3311} + 5\rho_{3333})\right\} \quad (7)$$

Based on the obtained averaged values, it is possible to estimate the concentration and mobility for charge carriers in that alloy. For this, the following simple formulas are used:

$$\left.\frac{1}{\rho} = eN\mu\left(\frac{1+b}{b}\right);\; R = \frac{1}{eN}\left(\frac{1-b}{1+b}\right);\; \frac{\delta\rho}{R^2B^2} = \frac{b^2}{(b-1)^2}\right\} \quad (8)$$

Here N is the electron concentration; μ and ν are the electron mobilities and holes, respectively; b denotes the ratio of the electron-mobility to the holes one, that is, μ/ν. Of course, these formulas correspond to the case degeneracy of charge carriers and $N=P$. More realistic formulas which cause the nondegeneracy of charge carriers in our case, there are for example, in [16]. The results of calculations by formulas (8) are given in the Table 3.

It should be noted that the data given in table 3 are in fairly good agreement with the corresponding data obtained for thick (≈1μm) polycrystalline $Bi_{0.944}Sb_{0.056}$ thin films [1].

Table 3.

Kinetic coefficients of $Bi_{0.94}Sb_{0.06}$ alloy in the temperature range 78-300*K*.

T	*N*	μ	*v*
(K)	(m^{-3})	$(m^2/V{\cdot}s)$	$(m^2/V{\cdot}s)$
78	2.1×10^{23}	37.09	4.63
90	2.57×10^{23}	29.02	3.63
110	3.62×10^{23}	19.39	2.42
130	5.00×10^{23}	13.21	1.65
150	6.81×10^{23}	9.12	1.14
170	9.27×10^{23}	6.29	0.95
190	1.21×10^{24}	4.52	0.67
210	1.51×10^{24}	3.39	0.49
230	1.85×10^{24}	2.61	0.33
250	2.27×10^{24}	2.02	0.25
270	2.71×10^{24}	1.60	0.20
290	3.36×10^{24}	1.23	0.15
300	3.78×10^{24}	1.07	0.13

[1] *S. Tang* and *M.S. Dresselhaus.* J. Mater. Chem. 2014, *C***,** 2, pp. 4710-4726.

[2] *A. Nikolaeva, L. Konopko, T. Huber, P. Bodiul, I. Popov E. Moloshnik*. Journal of Electronic Materials., 2012, pp. 1- 4.

[3] *S. Tang and M. S. Dresselhaus.* Physical Review., 2012, B, 86, 075436.

[4] *B. Landschreiber, E. Gunes, G. Homm, C. Will, P. Tomeš, C. Rohner, A. Sesselmann, P. Klar, S. Paschen, E. Muller and S. Schlecht*. Journal of Elec. Materials, 2013, pp. 1-6.

[5] *S. Tang and M. S. Dresselhaus*. Nanoscale., 2012, 4, 7786-7790.

[6] *L. Fu and C. L. Kane*. Physical Review., 2007, B, 76, 045302.

[7] *D. Hsieh, D. Qian, L. Wray, Y. Xia, Y. S. Hor, R. Cava and M. Z. Hasan*. Nature., 2008, 452, pp. 970-974.

[8] *F. Nakamura, et al.,* 2011, Physical Review B, 84, 235308.

[9] *E.I. Rogacheva, A.A. Drozdova, O.N. Nashchekina, M.S. Dresselhaus and G. Dresselhaus*. Applied Physics Letters., 2009, 94, 202111-202113.

[10] *A.A. Musayev*. Galvanomagnetic effects, dispersion of helicon waves and scattering of charge carriers in the Bi-Sb alloys at 77÷300*K*. Dissertation thesis, Baku.,1981.

[11] *J. G. Hust.* Rev. Sci. Instrum., 1970, 41, pp. 622–624.

[12] *M. Vecchi, E. Mendez, M.S. Dresselhaus*. "Physics of semiconductors", Proceedings of the 13-th International Conference., Rome. 1976, pp. 459-462.

[13] *K. Malik* et al. Journal of Applied Physic., 2012, 112, 083706.

[14] *E.I. Rogacheva, A.N. Doroshenko & O.N. Nashchekina.* Materials Today: Proceedings., 2021, 44, pp. 3458-3462.

[15] *A.A. Musayev, E.R. Yuzbashov.* Micro- and nanotechnologies in electronics. Proc. XI International scientific-technical conference. Nalchik, 3-8 June 2019. Nalchik: Kab.Balk. University., 2019, pp.126-130.

[16] *B.M. Askerov*. Electron transport phenomena in semiconductors. Moscow: "Nauka", 1985